2-15-1985

# Antireflecting and polarizing transparent bilayer coatings on absorbing substrates at oblique incidence

R. M.A. Azzam
*University of New Orleans*, razzam@uno.edu

Karim Javily

# Antireflecting and polarizing transparent bilayer coatings on absorbing substrates at oblique incidence

R. M. A. Azzam and Karim Javily

The condition of zero reflection of $p$- and $s$-polarized light by a transparent bilayer on an absorbing substrate is derived in the form $|g_\nu(\phi,N_i)| \leq 1$, where $g_\nu$ is a function of the angle of incidence $\phi$, the refractive indices $N_i$ ($i = 0,1,2,3$) of the system, and the polarization state $\nu$ ($= p$ or $s$). As an application, the air–$Si_3N_4$–$SiO_2$–Si system is considered at two laser wavelengths $\lambda = 6328$ and 3250 Å. The thicknesses of the two films of the bilayer and the unextinguished reflectance are determined as functions of $\phi$, and the results appear graphically and in tables. Extinction of the $s$ polarization is accompanied by low overall residual reflectance (e.g., for incident unpolarized light, it is 1.6% for $\lambda = 6328$ Å at $\phi = 45°$). On the other hand, suppression of the $p$ polarization at a high incidence angle is accompanied by high $s$ reflectance (e.g. = 96% for $\lambda = 3250$ Å at $\phi = 83°$). This demonstrates that efficient bilayer reflection polarizers are possible.

## I. Introduction

Antireflection coatings (ARCs) that consist of a stack of two transparent thin films on a transparent (dielectric) substrate at normal incidence are discussed in several reviews[1–3] and have attracted renewed attention recently.[4–6] Transparent bilayer (or double-layer) ARCs on a dielectric (glass) substrate for the parallel $p$ and perpendicular $s$ polarizations at 45° angle of incidence have been described by Turbadar.[7]

In this paper we consider transparent bilayer ARC on an absorbing substrate for the $p$ and $s$ polarizations as a function of the angle of incidence. A new derivation of the bilayer antireflection condition is developed (Sec. II) and is applied to the air–$Si_3N_4$–$SiO_2$–Si system at the (He–Ne laser) wavelength $\lambda = 6328$ Å at angles from normal to grazing incidence (Secs. III and IV). For the silicon substrate, the selection of its oxide and nitride films as the ARC materials is most logical and is consistent with the recently reported excellent optical characteristics of such films.[8,9] The same system is also considered at a shorter (He–Cd laser) UV wavelength, $\lambda = 3250$ Å, where Si becomes highly absorbing and behaves like a metal (Sec. V). In this case, antireflection of the $p$ polarization is possible at high angles of incidence and is accompanied by high reflectance (~96%) for the unextinguished $s$ polarization. Therefore, an efficient bilayer reflection polarizer is obtained.

The authors are with University of New Orleans, Department of Electrical Engineering, Lakefront, New Orleans, Louisiana 70148.

Received 22 October 1984.
0003-6935/85/040519-08$02.00/0.



## II. Antireflection Conditions for a Transparent Bilayer on an Absorbing Substrate at Oblique Incidence

The following derivation of the antireflection conditions of $p$- and $s$-polarized light by a transparent bilayer–substrate system differs from the often-quoted treatment by Catalan[10] analytically, and in that the substrate may be absorbing (e.g., semiconductor or metallic) instead of being dielectric.

We consider the oblique-incidence reflection at an angle $\phi$ of monochromatic light of wavelength $\lambda$ traveling in an ambient (medium 0, usually air) by a system of two transparent thin films (film 1 and film 2) on an absorbing substrate (medium 3). All (bulk and thin-film) media are assumed to be homogeneous, optically isotropic, linear, and nonmagnetic and are separated by sharp parallel–plane interfaces. The complex-amplitude reflection coefficients of such a system are given by[11]

$$R_\nu = \frac{r_{01\nu} + r_{12\nu}X_1 + r_{01\nu}r_{12\nu}r_{23\nu}X_2 + r_{23\nu}X_1X_2}{1 + r_{01\nu}r_{12\nu}X_1 + r_{12\nu}r_{23\nu}X_2 + r_{01\nu}r_{23\nu}X_1X_2}, \quad \nu = p,s, \tag{1}$$

where

$$X_i = \exp(-j2\pi\zeta_i), \qquad i = 1,2, \tag{2}$$

and $r_{lm\nu}$ is Fresnel's reflection coefficient of the $lm$ interface for the $\nu$ polarization. (Such coefficients are given elsewhere[12,13] and will not be repeated here.) In Eq. (2), $\zeta_i$ is the normalized thickness of the $i$th film,

$$\zeta_i = d_i/D_{\phi i}, \qquad i = 1,2, \tag{3}$$

where $d_i$ is the actual (metric) thickness, $D_{\phi i}$ is the associated film thickness period,

$$D_{\phi i} = \frac{\lambda}{2}(N_i^2 - N_0^2 \sin^2\phi)^{-1/2}, \qquad i = 1,2. \tag{4}$$

$N_i$ is the refractive index of the $i$th medium ($i = 0,1,2,3$). The ambient and two films are transparent, so that $N_0$, $N_1$, and $N_2$ are real, whereas the substrate is in general absorbing and is characterized by a complex refractive index $N_3 = n_3 - jk_3$.

Extinct reflection of the $\nu$ polarization occurs when the numerator of Eq. (1) is zero, i.e.,

$$r_{01\nu} + r_{12\nu}X_1 + r_{01\nu}r_{12\nu}r_{23\nu}X_2 + r_{23\nu}X_1X_2 = 0. \tag{5}$$

Equation (5) can be rearranged to read

$$X_2 = (A_\nu + B_\nu X_1)/(C_\nu + X_1), \tag{6}$$

where

$$A_\nu = -r_{01\nu}/r_{23\nu}, \quad B_\nu = -r_{12\nu}/r_{23\nu}, \quad C_\nu = r_{01\nu}r_{12\nu}. \tag{7}$$

If we substitute

$$X_i = \exp(-j\theta_i), \quad \theta_i = 2\pi\zeta_i, \quad i = 1,2, \tag{8a}$$

$$A_\nu = a_\nu \exp(j\alpha_\nu), \quad B_\nu = b_\nu \exp(j\beta_\nu), \quad C_\nu = c_\nu \exp(j\gamma_\nu), \tag{8b}$$

into Eq. (6) and equate the absolute value of both sides to 1, we get

$$G_{1\nu}\cos\theta_1 + G_{2\nu}\sin\theta_1 = G_{0\nu}, \tag{9}$$

where

$$G_{0\nu} = c_\nu^2 - b_\nu^2 - a_\nu^2 + 1, \tag{10a}$$

$$G_{1\nu} = 2a_\nu b_\nu \cos(\alpha_\nu - \beta_\nu) - 2c_\nu \cos\gamma_\nu, \tag{10b}$$

$$G_{2\nu} = -2a_\nu b_\nu \sin(\alpha_\nu - \beta_\nu) + 2c_\nu \sin\gamma_\nu. \tag{10c}$$

Because the two films are transparent, the interface reflection coefficients $r_{01\nu}, r_{12\nu}$ are real (total internal reflection is, of course, excluded), and from Eqs. (7) and (8b) it follows that

$$\alpha_\nu - \beta_\nu = 0 \text{ or } \pm\pi, \gamma_\nu = 0 \text{ or } \pm\pi. \tag{11}$$

Substitution of Eqs. (11) into Eq. (10c) indicates that

$$G_{2\nu} = 0, \tag{12}$$

and Eq. (9) simplifies to

$$\cos\theta_1 = G_{0\nu}/G_{1\nu} = g_\nu. \tag{13}$$

Equation (13) has a real solution for $\theta_1$ if

$$|g_\nu| \le 1. \tag{14}$$

Equations (7), (8b), (10a), (10b), and (13) indicate that $g_\nu$ is a function of the 01, 12, and 23 interface reflection coefficients for the $\nu$ polarization; hence $g_\nu$ is a function of the refractive indices $N_0,N_1,N_2,N_3$ and angle of incidence $\phi$, i.e.,

$$g_\nu = f(N_0,N_1,N_2,N_3,\phi). \tag{15}$$

For given optical constants $N_i$ ($i = 0,1,2,3$) of a given ambient–bilayer–substrate system, $g_\nu$ can be computed as a function of $\phi$ for the $\nu = p,s$ polarizations. Only over those ranges of $\phi$ for which Eq. (14) is satisfied is the extinction of $\nu$-polarized light possible. With $|g_\nu| \le 1$, Eq. (13) has two solutions for $\theta_1$ in the range $0 \le \theta_1 < 2\pi$:

$$\theta_{1a} = \cos^{-1} g_\nu, \quad 0 \le \theta_{1a} < \pi,$$

$$\theta_{1b} = 2\pi - \theta_{1a}. \tag{16}$$

Other solutions, obtained by adding integral multiples of $2\pi$ to $\theta_1$, will be ignored.

Once $\theta_{1a,b}$ are determined, Eq. (6) is used to determine $X_{2a,b}$ and the corresponding $\theta_{2a,b}$:

$$\theta_{2a,b} = -\arg X_{2a,b}, \qquad 0 \le \theta_{2a,b} < 2\pi. \tag{17}$$

The two solution pairs of the least ($0 \le \zeta_i < 1, i = 1,2$) normalized film thicknesses are

$$(\zeta_1,\zeta_2)_{a,b} = \frac{1}{2\pi}(\theta_1,\theta_2)_{a,b}, \tag{18}$$

and the corresponding (least) actual film thicknesses are obtained by multiplying $\zeta_1$ and $\zeta_2$ by the corresponding thickness periods $D_{\phi 1}, D_{\phi 2}$ [Eqs. (3) and (4)].

The intensity reflectances for the extinguished and orthogonal (passed) polarizations are subsequently calculated from

$$\mathcal{R}_\nu = |R_\nu|^2, \tag{19}$$

where $R_\nu$ is given by Eq. (1). Of course, the extinguished reflectance should be zero, or virtually so (e.g., $<10^{-6}$), and its calculation serves as a check. If the passed reflectance is also very small (of the order of a few percent or less), the bilayer acts as an efficient overall antireflection stack. On the other hand, if the passed reflectance is high (say >80%), the bilayer becomes an efficient polarizer.

## III. s-Polarization–Antireflection $Si_3N_4$–$SiO_2$ Bilayers on Si at $\lambda = 6328$ Å

The refractive indices of $Si_3N_4$, $SiO_2$, and Si at $\lambda = 6328$ Å are taken as $N_1 = 1.98$, $N_2 = 1.46$, and $N_3 = 3.85 - j0.02$, respectively,[14] and the medium of incidence is assumed to be air, $N_0 = 1$.

Figure 1 shows $|g_s(\phi)|$ vs $\phi$ computed from Eqs. (7), (8b), (10a), (10b), and (13). Suppression of the reflection of the $s$ polarization by the $Si_3N_4$–$SiO_2$ bilayer on Si is possible at angles of incidence from 0 (normal incidence) up to a maximum angle $\phi_s = 70.56°$. Over this range, $0 \le \phi < \phi_s$, $|g_s| < 1$, and at $\phi = \phi_s$, $|g_s| = 1$, so that Eq. (14) is satisfied.

Figure 2(a) shows the solution pair $a$ of nitride and oxide (least) normalized film thicknesses $\zeta_{1a},\zeta_{2a}$ as functions of $\phi$ computed from Eqs. (16)–(18). The associated actual film thicknesses $d_{1a},d_{2a}$ in Å appear in Fig. 2(b). At $\phi = \phi_s, g_s = 1, \theta_{1a} = 0$ from Eq. (16), and we have $\zeta_{1a} = d_{1a} = 0$; thus $s$-polarization antireflection is possible with an oxide layer only whose normalized and actual thicknesses[15] are $\zeta_{2a} = 0.499424$, $d_{2a} = 1417.7$ Å. The intersection points $E$ in Figs. 2(a) and (b) indicate that $s$ antireflection with two layers of equal normalized thicknesses ($\zeta \simeq 0.21$) occurs at an angle between 54 and 55° and with layers of equal actual thicknesses ($d \simeq 435$ Å) at an angle between 47 and 48°.

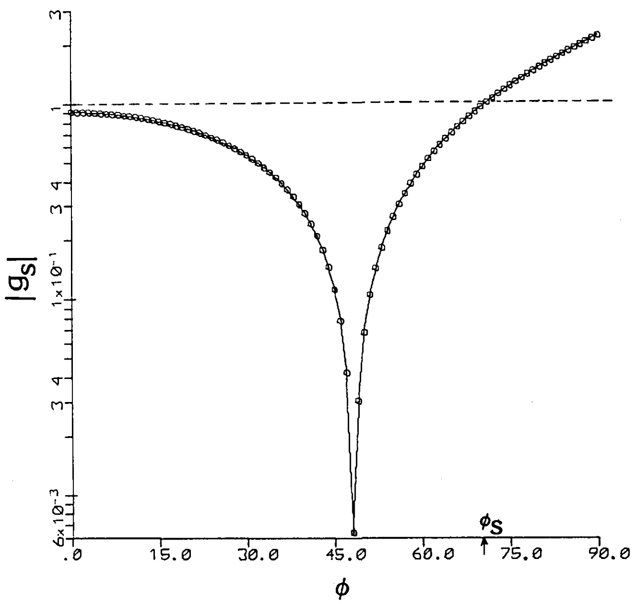


Fig. 1. Graph of the function $|g_s(\phi)|$ vs angle of incidence $\phi$. Zero reflection for the $s$ polarization occurs over the range $0 \leq \phi \leq \phi_s$, where $|g_s(\phi)| \leq 1$. We assume the air–$Si_3N_4$–$SiO_2$–Si system at wavelength $\lambda = 6328$ Å.

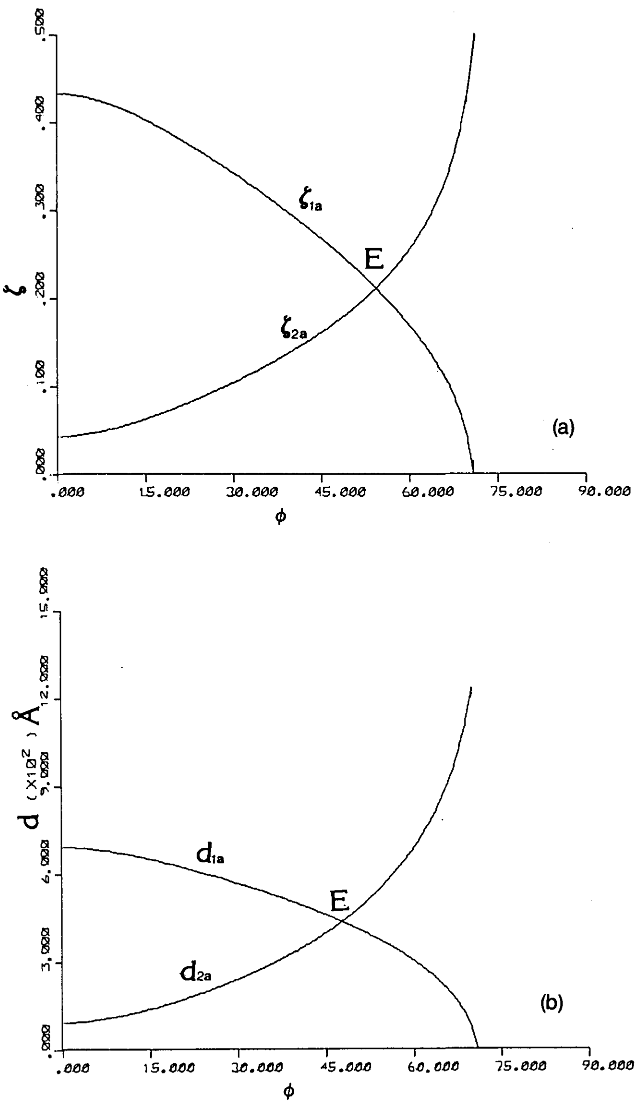


Fig. 2. (a) Normalized film thicknesses of the nitride $\zeta_{1a}$ and oxide $\zeta_{2a}$ layers on Si required for zero reflection of the $s$ polarization ($\lambda$ = 6328 Å) as functions of the angle of incidence $\phi$. This is solution $a$ of two solutions denoted $a$ and $b$. (b) The corresponding actual film thicknesses $d_{1a}$ and $d_{2a}$ in angstroms.

Figures 3(a) and (b) present the normalized and actual layer thicknesses, $(\zeta_{1b},\zeta_{2b})$ and $(d_{1b},d_{2b})$, respectively, for the second independent solution pair $b$ vs angle of incidence $\phi$. Whereas $\zeta_{1b} = 1 - \zeta_{1a}$ [from Eqs. (16) and (18)], $\zeta_{2b} \neq 1 - \zeta_{1b}$ because the substrate is absorbing. However, the small extinction coefficient of Si ($k_3 = 0.02$) makes the approximate relation $\zeta_{2b} \simeq 1 - \zeta_{1b}$ valid. As indicated by intersection points $E$, $s$ antireflection with equal normalized layer thicknesses ($\zeta \simeq 0.79$) occurs at $\phi$ between 54 and 55°, and its occurs with equal actual layer thicknesses ($d \simeq 1700$ Å) at $\phi \simeq 69°$.

An important observation from Fig. 3(b) is that the (inner) oxide-layer thickness $d_{2b}$ stays nearly constant (between 2050 and 2080 Å), and the $s$-polarizing angle $\phi$ varies over a wide range (from 0 to 55°) by changing the thickness of the top nitride layer from ~900 to 1400 Å. Measuring $\phi$ provides a simple and convenient means of controlling the thickness of the $Si_3N_4$ film (over a 500-Å range) on the underlying Si wafer, which is oxidized to a thickness of ~2065 Å. It is perhaps worthwhile to look for similar characteristics of this (and other) double-layer systems at several wavelengths, which may be useful in film-thickness metrology.

Figure 4 shows the monotonic rise of the unextinguished reflectance $\mathcal{R}_p$ [calculated from Eq. (19)] with the polarizing angle $\phi$ from 0 at $\phi = 0$ to 28% at $\phi = \phi_s = 70.56°$. Both solutions $a$ and $b$ lead to coincident curves of $\mathcal{R}_p$.

Table I summarizes data for $s$-polarization–antireflection $Si_3N_4$–$SiO_2$ bilayers on Si at five angles of incidence $\phi$ = 0, 30, 45, 60, and 70° for the wavelength $\lambda$ = 6328 Å. The low unextinguished reflectances $\mathcal{R}_p$ of 0.59 and 3.2% at $\phi$ = 30 and 45°, respectively, indicate excellent overall antireflection behavior at these angles. Because $\mathcal{R}_s = 0$, the residual reflectance for incident unpolarized light equals $\frac{1}{2}\mathcal{R}_p$, i.e., = 0.3 and 1.6% at 30 and 45°, respectively. The highest attainable reflectance ($\mathcal{R}_p$ = 28% at $\phi$ = 70.56°) is not high enough to make this bilayer–substrate system function as an efficient polarizer.

## IV. *p*-Polarization–Antireflection $Si_3N_4$–$SiO_2$ Bilayers on Si at $\lambda$ = 6328 Å

The method of Sec. II, which was applied to $s$-polarization antireflection in Sec. III, is applied in this section to $p$-polarization antireflection by the same nitride–oxide–silicon system at the same He–Ne laser wavelength $\lambda$ = 6328 Å.

Figure 5 shows $|g_p(\phi)|$ plotted as a function of $\phi$ from normal ($\phi = 0$) to grazing ($\phi = 90°$) incidence. This curve intersects the line $|g_p| = 1$ at three points $Q_1$,$Q_2$,

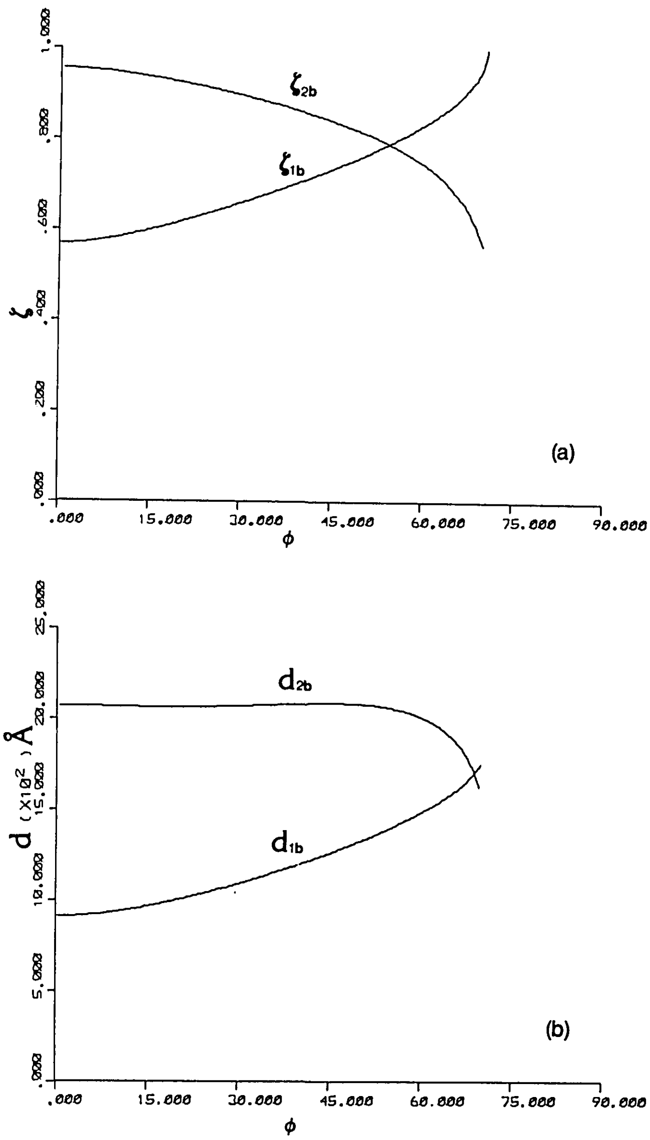


Fig. 3. (a) Normalized film thicknesses of the nitride $\zeta_{1b}$ and oxide $\zeta_{2b}$ layers on Si required for zero reflection of the $s$ polarization ($\lambda$ = 6328 Å) as functions of the angle of incidence $\phi$. This is solution $b$ of two solutions denoted $a$ and $b$. (b) The corresponding actual film thicknesses $d_{1b}$ and $d_{2b}$ in angstroms.

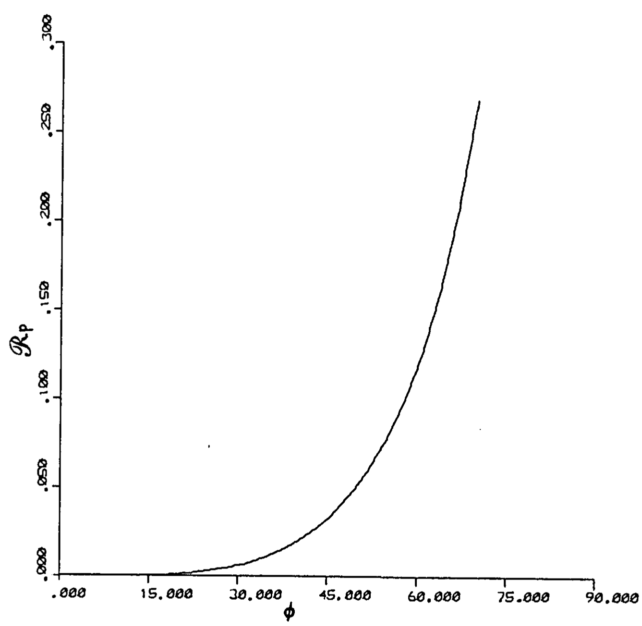


Fig. 4. Unextinguished reflectance for the $p$ polarization $\mathcal{R}_p$ as a function of angle of incidence $\phi$ for a $Si_3N_4$–$SiO_2$ bilayer on Si that suppresses the reflection of $s$-polarized incident light ($\lambda$ = 6328 Å).

**Table I. Characteristics of $Si_3N_4$–$SiO_2$ Bilayer Antireflection Coatings on Si for the $s$ Polarization at $\lambda$ = 6328 Å [a]**

| $\phi$ (deg) | $\zeta_1$ | $\zeta_2$ | $d_1$ (Å) | $d_2$ (Å) | $\mathcal{R}_p$ (%) |
|---|---|---|---|---|---|
| 0 | 0.4317 | 0.0431 | 689.9 | 93.3 | 0 |
| | 0.5683 | 0.9555 | 908.1 | 2070.6 | 0 |
| 30 | 0.3422 | 0.1033 | 565.2 | 238.2 | 0.59 |
| | 0.6578 | 0.8954 | 1086.3 | 2065.2 | 0.59 |
| 45 | 0.2679 | 0.1596 | 458.3 | 395.4 | 3.20 |
| | 0.7321 | 0.8391 | 1252.5 | 2078.4 | 3.20 |
| 60 | 0.1703 | 0.2533 | 302.6 | 681.9 | 11.85 |
| | 0.8297 | 0.7455 | 1474.4 | 2006.6 | 11.83 |
| 70 | 0.0391 | 0.4354 | 71.0 | 1232.8 | 26.91 |
| | 0.9609 | 0.5635 | 1744.5 | 1595.5 | 26.90 |

[a] $\phi$ is the angle of incidence. $\zeta_1$,$\zeta_2$ are the normalized, whereas $d_1$,$d_2$ are the actual, $Si_3N_4$,$SiO_2$ film thicknesses, respectively. $\mathcal{R}_p$ is the unextinguished reflectance for the $p$ polarization. At each angle, two solutions are given; that on the upper line is denoted $a$ in the text, lower line is for solution $b$. The refractive indices of $Si_3N_4$,$SiO_2$, and Si are 1.98, 1.46, and 3.85–$j$0.02, respectively, at $\lambda$ = 6328 Å. Air is the medium of incidence.

and $Q_3$. Antireflection is possible only when $|g_p| \le 1$, Eq. (14), i.e., over two disconnected angular ranges:

$$\text{(I)} \quad 0 \le \phi \le \phi_{p1} = 14.39°,$$

$$\text{(II)} \quad 75.44° = \phi_{p2} \le \phi \le \phi_{p3} = 79.16°.$$

($\phi_{pk}$ corresponds to the $k$th intersection point $Q_k$, $k$ = 1,2,3). We now examine the solutions obtained over each of these ranges.

The normalized ($\zeta_{1a}$,$\zeta_{2a}$) and actual ($d_{1a}$,$d_{2a}$) thicknesses of the (nitride,oxide) bilayer for $R_p = 0$ are given as functions of $\phi$ over range I in Figs. 6(a) and (b) and over range II in Figs. 6(c) and (d), respectively, for solution pair $a$. As $\phi$ increases from 0 to $\phi_{p1}$ = 14.39°, $\zeta_{2a}$ decreases from 0.0431 to 0, while $\zeta_{1a}$ increases from 0.4317 to 0.4989, both monotonically, as shown in Fig. 6(a). At $\phi_{p1}$, $R_p = 0$ is accomplished by the (803.5-Å) nitride layer alone. Figures 6(c) and (d) show that at $\phi_{p2}$ = 75.44°, $\zeta_{1a} = d_{1a} = 0$, and $p$ antireflection is possible with an oxide layer alone whose normalized and actual thicknesses are $\zeta_{2a}$ = 0.999 and $d_{2a}$ = 2891.7 Å. As $\phi$ is increased from $\phi_{p2}$ to $\phi_{p3}$ = 79.16°, $\zeta_{1a}$ increases, and $\zeta_{2a}$ decreases, merging to a common value of 0.5 (i.e., both layers become essentially quarterwaves at the upper limit $\phi_{p3}$).

Solution pair $b$ is represented in a similar fashion by Fig. 7. Figures 7(a) and (b) show that ($\zeta_{1b}$,$\zeta_{2b}$) and ($d_{1b}$,$d_{2b}$) vary little with $\phi$ over range I. Figure 7(c) shows that $\zeta_{2b}$ = 0 at $\phi_{p2}$ = 75.44°, so that $R_p$ = 0 can be achieved by a nitride layer alone of thickness just less than one full thickness period. Here, as in Fig. 6, $\zeta_{1b}$,$\zeta_{2b}$

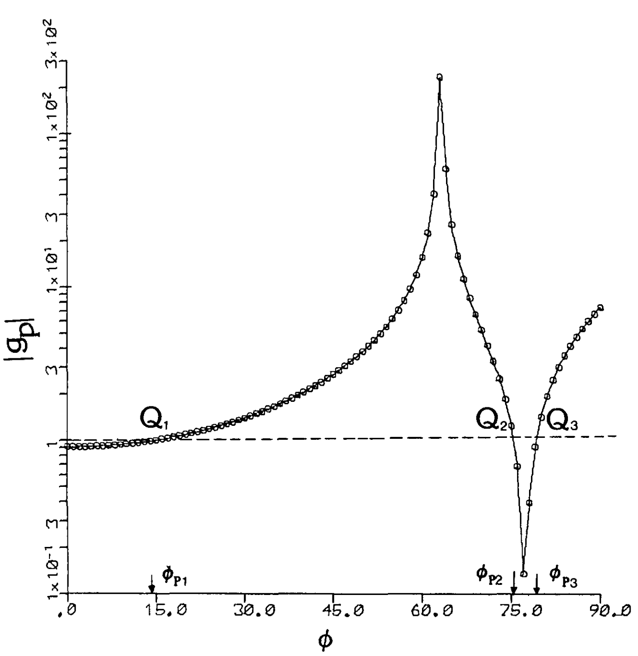


Fig. 5. Graph of the function $|g_p(\phi)|$ vs angle of incidence $\phi$. The points of intersection $Q_1$, $Q_2$, and $Q_3$ of the curve with the straight line $|g_p| = 1$ define two ranges $0 \leq \phi \leq \phi_{p1}$ and $\phi_{p2} \leq \phi \leq \phi_{p3}$ over which zero reflection for the $p$ polarization is possible by the air–$Si_3N_4$–$SiO_2$–Si system at $\lambda = 6328$ Å.

$\rightarrow 0.5$ as $\phi \rightarrow 79.16°$. Figure 7(c) shows that $p$ antireflection is realized with a bilayer of equal nitride and oxide thicknesses ($d = 1102$ Å) at $\phi = 78.8°$.

Finally, Fig. 8 gives the unextinguished reflectance $\mathcal{R}_s$ as a function of $\phi$ over angular ranges I and II. (Both solutions $a$ and $b$ lead to nearly identical reflectance curves.) Figure 8(a) shows a small parabolic increase of $\mathcal{R}_s$ from 0 to $\simeq 0.03\%$ between $\phi = 0$ and $\phi = 14.39°$. Obviously, we have an excellent angle-insensitive normal-incidence antireflection bilayer on Si. On the other hand, Fig. 8(b) shows that $\mathcal{R}_s$ is high and increases[16] monotonically with $\phi$ from 76.32% (at $\phi = 75.44°$) to 92.33% (at $\phi = 79.16°$). Over this range of high angles, the $Si_3N_4$–$SiO_2$–Si system acts as an efficient reflection polarizer for $\lambda = 6328$-Å light.

Table II summarizes data for $R_p = 0$ bilayer reflection polarizers at $\phi = 77$ and 79°.

## V. Efficient $R_p = 0$ $Si_3N_4$–$SiO_2$–Si Reflection Polarizers at $\lambda = 3250$ Å

At the shorter UV wavelength $\lambda = 3250$ Å, the refractive indices of $Si_3N_4$, $SiO_2$, and Si are 2.01, 1.482, and $5.063 - j3.218$, respectively.[17,18] The latter complex refractive index indicates that Si behaves effectively as a metal, and such a bilayer–substrate system becomes, in general, more highly reflecting.

We find that suppression of the reflection of $p$-polarized light is possible within a narrow interval of angles, $82.16° \leq \phi \leq 84.15°$, and impossible outside. As $\phi$ increases from its lower (82.16°) to its upper (84.15°) limit, the unextinguished reflectance $\mathcal{R}_s$ increases monotonically from 92.73 to 97.78%, so that a highly efficient reflection polarizer is achieved. We now quote the characteristics of one such polarizer operating at $\phi = 83°$. The normalized and actual layer thicknesses are given by

$$(\zeta_{1a},\zeta_{2a}) = (0.2265, 0.7408),$$

$$(\zeta_{1b},\zeta_{2b}) = (0.7735, 0.1407),$$

$$(d_{1a},d_{2a}) = (210.5, 1093.8)\ \text{Å},$$

$$(d_{1b},d_{2b}) = (718.6, 207.7)\ \text{Å}.$$

These thicknesses indicate that $\zeta_{1a} + \zeta_{1b} = 1$, as before, whereas $\zeta_{2a} + \zeta_{2b}$ (= 0.8815) is now significantly different from 1 because of the high extinction coefficient of the Si substrate ($k_3 = 3.218$). It is also interesting to note that solution $b$ leads to a smaller (926.3-Å) overall thickness of the bilayer than does solution $a$ (1304.3 Å). The unextinguished $s$ reflectances associated with solutions $a$ and $b$ are 95.77 and 95.32%, respectively. The difference between $\mathcal{R}_{sa}$ and $\mathcal{R}_{sb}$, although still small (0.45%), is perceptible with a highly absorbing substrate.

## VI. Summary

In this paper we have presented a simple fresh derivation of the conditions of zero reflection of $p$- and $s$-polarized light by a transpare bilayer on an absorbing substrate with the angle of incidence $\phi$ considered as an independent variable. Prior work was limited to transparent substrates at normal or 45° oblique incidence. We applied our method to the important and attractive $Si_3N_4$–$SiO_2$ double layer on Si at two laser wavelengths $\lambda = 6328$ and 3250 Å. Antireflection of the $p$ or $s$ polarization is possible over limited ranges of $\phi$ and only for certain combinations of the individual layer thicknesses.

Antireflection of the $s$ polarization is accompanied by a low residual $p$ reflectance $\mathcal{R}_p$ that increases with $\phi$. For example, for the air–$Si_3N_4$–$SiO_2$–Si system at $\lambda = 6328$ Å, $\mathcal{R}_p = 0.59$ and 3.2% at $\phi = 30$ and 45°, respectively. The corresponding reflectances for unpolarized incident light are $\mathcal{R}_u = \frac{1}{2}\mathcal{R}_p = 0.3$ and 1.6%. Thus excellent overall antireflection at oblique incidence is attainable. On the other hand, zero reflection for the $p$ polarization at a high angle of incidence is accompanied by a high unextinguished reflectance $\mathcal{R}_s$. For example, for the same nitride–oxide–silicon system we find that, when $R_p = 0$, $\mathcal{R}_s = 91.92\%$ at $\phi = 79°$, $\lambda = 6328$ Å, and $\mathcal{R}_s = 95.77\%$ at $\phi = 83°$, $\lambda = 3250$ Å. Therefore, efficient bilayer reflection polarizers are realizable.

A useful interesting byproduct of this study is the finding that if the Si substrate is oxidized until the $SiO_2$ layer thickness is ~2065 Å, $s$-polarization antireflection will occur at an angle that depends solely on the $Si_3N_4$ top-layer thickness. Measurement of such angle (which varies from 0 to 55°) determines the nitride-layer thickness (in the 900–1400-Å range).

This work was supported by the State of Louisiana Board of Regents and the Foundation for A Better Louisiana.

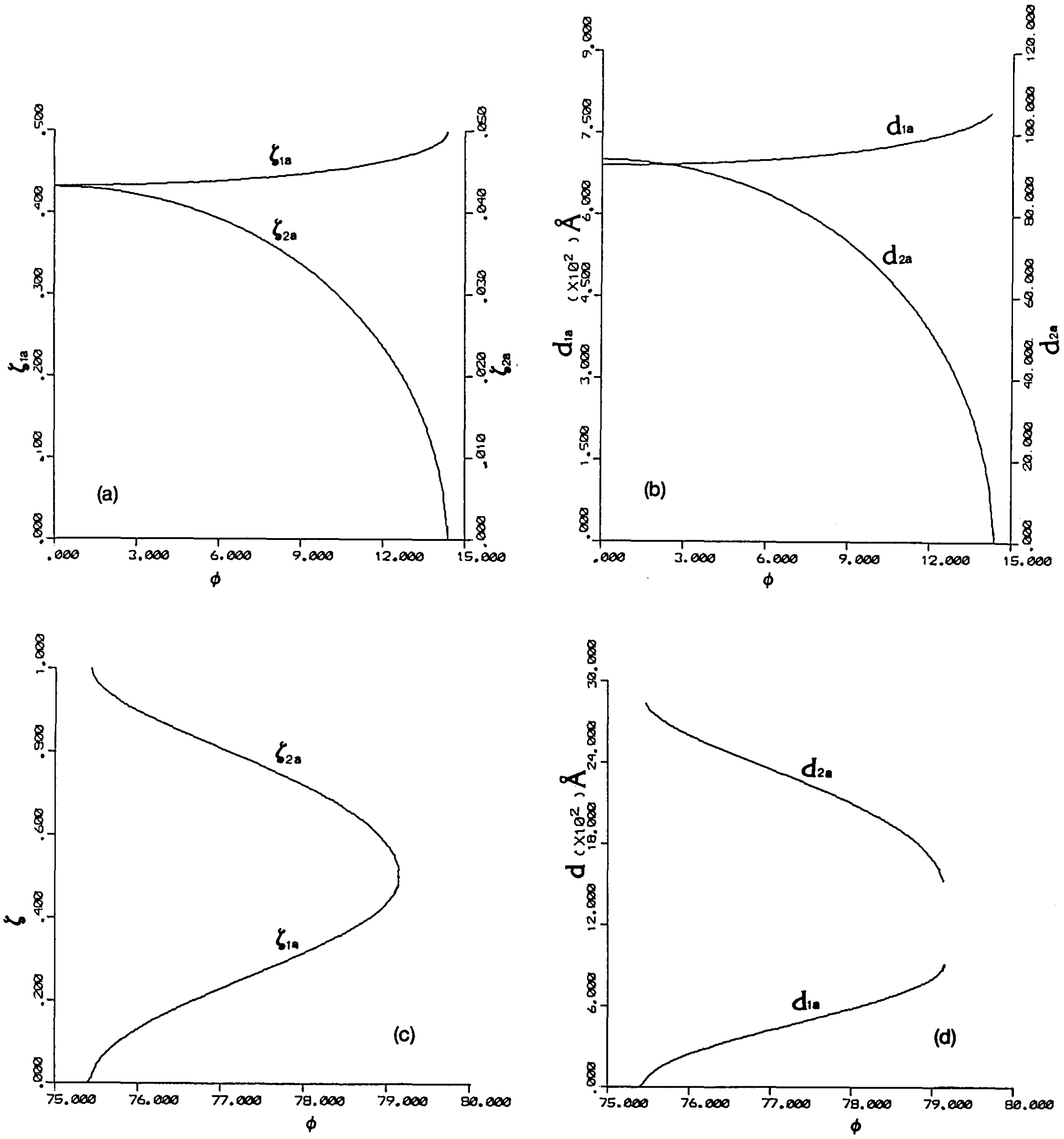


Fig. 6. (a), (c) Normalized film thicknesses of the nitride $\zeta_{1a}$ and oxide $\zeta_{2a}$ layers on Si required for zero reflection of the $p$ polarization ($\lambda$ = 6328 Å) as functions of the angle of incidence $\phi$. This is solution $a$ of two solutions denoted $a$ and $b$. (b), (d) Corresponding actual film thicknesses $d_{1a}$ and $d_{2a}$ in angstroms.

**Table II. Characteristics of $p$-Suppressing $Si_3N_4$-$SiO_2$-Si Reflection Polarizers at Two Angles of Incidence and $\lambda$ = 6328 Å [a]**

| $\phi$ (deg) | $\zeta_1$ | $\zeta_2$ | $d_1$ (Å) | $d_2$ (Å) | $\mathcal{R}_s$ (%) |
|---|---|---|---|---|---|
| 77 | 0.2283 | 0.8090 | 419.2 | 2354.1 | 84.93 |
| | 0.7717 | 0.1890 | 1416.5 | 550.1 | 84.91 |
| 79 | 0.4345 | 0.5804 | 799.4 | 1699.3 | 91.92 |
| | 0.5655 | 0.4175 | 1040.6 | 1222.4 | 91.91 |

[a] $\phi$ is the angle of incidence. $\zeta_1,\zeta_2$ are the normalized, whereas $d_1,d_2$ are the actual, $Si_3N_4$,$SiO_2$ film thicknesses, respectively. $\mathcal{R}_s$ is the unextinguished reflectance for the $s$ polarization. At each angle, two solutions are given; that on the upper line is denoted $a$ in the text, lower line is for solution $b$. The refractive indices of $Si_3N_4$,$SiO_2$, and Si are 1.98, 1.46, and 3.85–$j$0.02, respectively, at $\lambda$ = 6328 Å. Air is the medium of incidence.

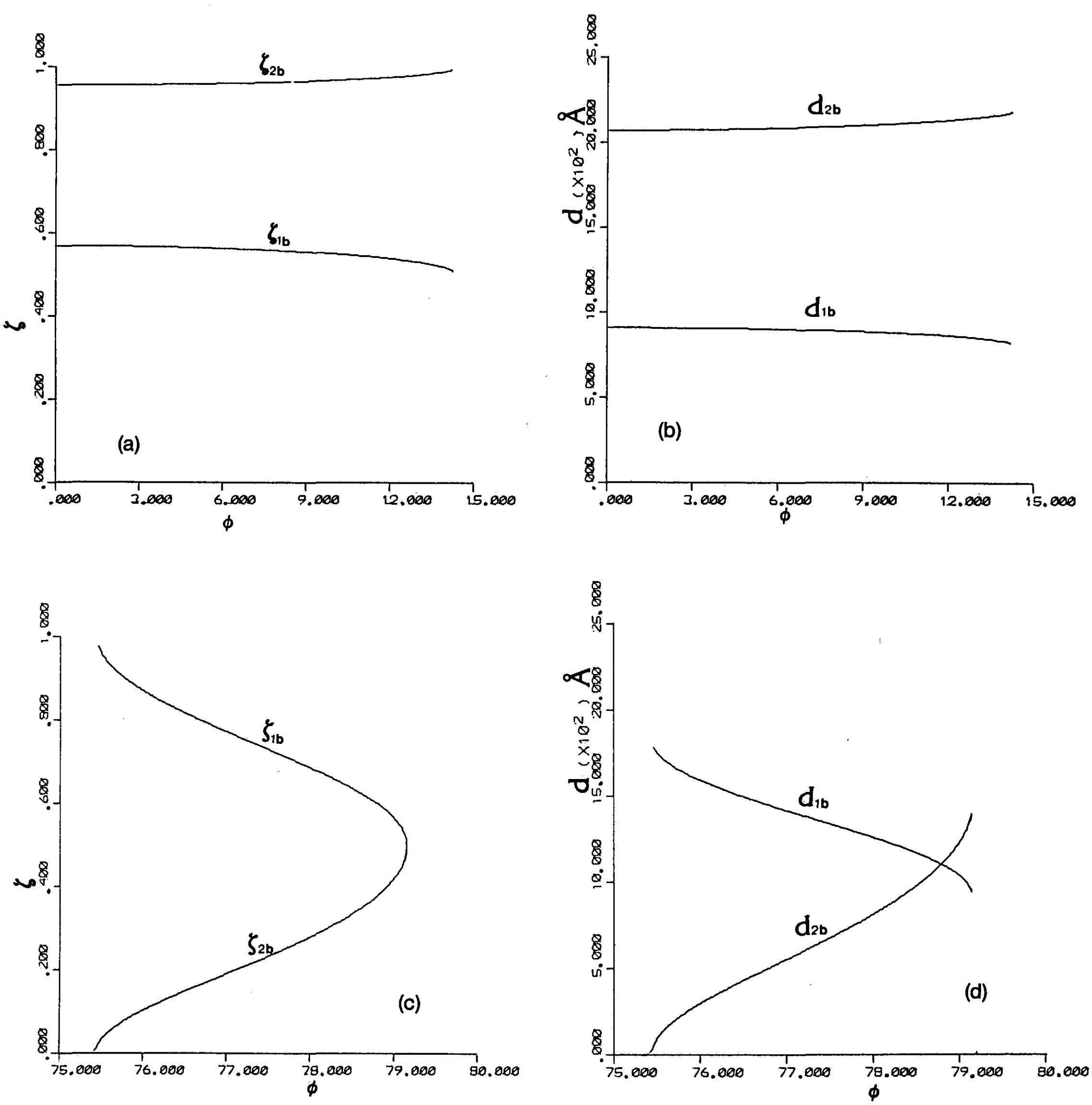


Fig. 7. (a), (c) Normalized film thicknesses of the nitride $\zeta_{1b}$ and oxide $\zeta_{2b}$ layers on Si required for zero reflection of the $p$ polarization ($\lambda$ = 6328 Å) as functions of the angle of incidence $\phi$. This is solution $b$ of two solutions denoted $a$ and $b$. (b), (d) Corresponding actual film thickness $d_{1b}$ and $d_{2b}$ in angstroms.

## References


1. J. T. Cox and G. Hass, "Antireflection Coatings for Optical and Infrared Optical Materials," in *Physics of Thin Films, Vol. 2*, G. Hass and R. E. Thun, Eds. (Academic, New York, 1964).
2. A. Musset and A. Thelen, "Multilayer Antireflection Coatings," in *Progress in Optics, Vol. 8*, E. Wolf, Ed. (North-Holland, Amsterdam, 1970).
3. J. A. Dobrowolski, "Coatings and Filters," in *Handbook of Optics*, W. G. Driscoll and W. Vaughan, Eds. (McGraw-Hill, New York, 1978).
4. C. J. van der Laan and H. J. Frankena, "Production of High-Quality V-Coatings," Appl. Opt. **21**, 2809 (1982).
5. I. Lubezky, E. Ceren, Z. Taubenfeld, and H. Zipin, "Efficient and Durable AR Coatings for Ge in the 8–11.5-$\mu$m Band using Synthesized Refractive Indices by Evaporation of Homogeneous Mixtures," Appl. Opt. **22**, 1828 (1983).
6. I. Lubezky, and A. Lubezky, "Practical Design of Double-Layer Antireflection Coatings for High-Index Substrates," Opt. Eng. **22**, 753 (1983).
7. T. Turbadar, "Equi-reflectance Contours of Double-Layer Antireflection Coatings," Opt. Acta **11**, 159 (1964).
8. S. Sriram, W. D. Partlow, and C. S. Liu, "Low-Loss Optical Waveguides using Plasma-Deposited Silicon Nitride," Appl. Opt. **22**, 3664 (1983).
9. P. M. Martin, W. T. Pawlewicz, D. Coult, and J. Jones, "Observation of Exceptional Temperature Humidity Stability in Multilayer Filter Coatings," Appl. Opt. **23**, 1307 (1984).
10. L. A. Catalan, "Some Computed Optical Properties of Antireflection Coatings," J. Opt. Soc. Am. **52**, 437 (1962).
11. R. M. A. Azzam and N. M. Bashara, *Ellipsometry and Polarized Light* (North-Holland, Amsterdam, 1977), Eq. (4.185), p. 340. [Note that the following Eq. (4.186) should have the same denominator as Eq. (4.185). Similar comments apply to two unnumbered equations on p. 339. These corrections follow from replacing $S_{21}$ by $S_{11}$ in Eq. (4.170).]
12. R. M. A. Azzam and N. M. Bashara, *Ellipsometry and Polarized Light* (North-Holland, Amsterdam, 1977), Sec. 4.2.
13. M. Born and E. Wolf, *Principles of Optics* (Pergamon, New York, 1975), Sec. 1.5.

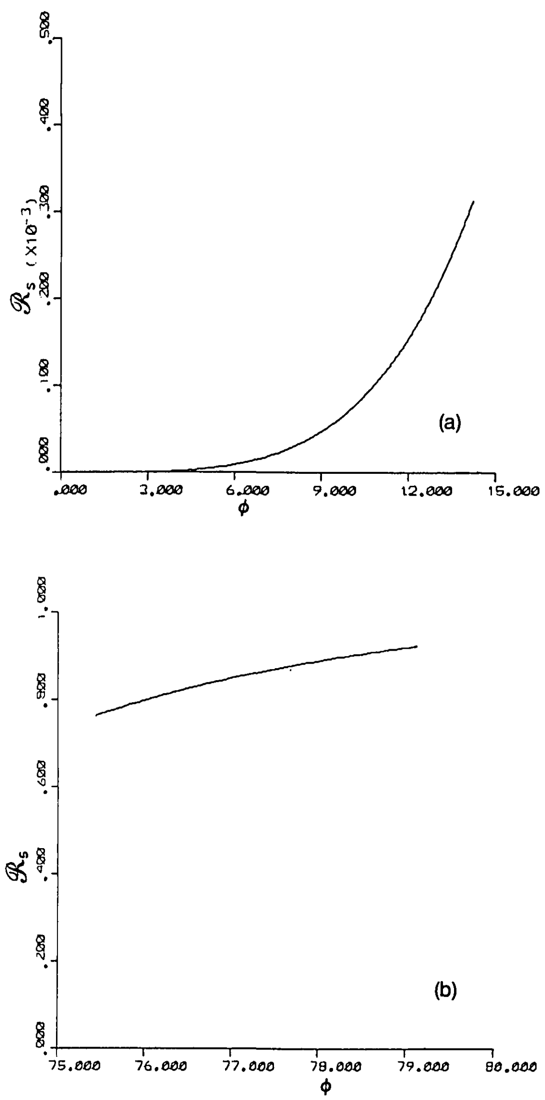


Fig. 8. Unextinguished reflectance for the $s$ polarization $\mathcal{R}_s$ as a function of angle of incidence $\phi$ over two separate ranges (a) and (b) for a $Si_3N_4$–$SiO_2$ bilayer on Si that suppresses the reflection of $p$-polarized incident light ($\lambda = 6328$ Å).


14. The refractive index $N_1 = 1.98$ is that of stoichiometric silicon nitride. See, e.g., G. Eisenstein and L. W. Stulz, "High Quality Antireflection Coatings on Laser Facets by Sputtered Silicon Nitride," Appl. Opt. **23,** 161 (1984). The refractive indices of $SiO_2$ and Si are obtained from G. Gergely, Ed., *Ellipsometric Tables of the Si–$SiO_2$ System for Mercury and He–Ne Laser Spectral Lines* (Akademiai Kiado, Budapest, 1971).
15. The deviation of $\zeta_{2a}$ from 0.5 is due to the small (0.02) but nonzero extinction coefficient of the Si substrate.
16. Such an enhancement of the unextinguished reflectance $\mathcal{R}_s$ (of up to 16%) represents the benefit of adding the second $Si_3N_4$ layer on top of the $SiO_2$–Si substructure, in as far as operation as a reflection polarizer is concerned.
17. A. J. Warnecke and P. J. LoPresti, "Refractive Index Dispersion in Semiconductor-Related Thin Films," IBM J. Res. Dev. **17,** 256 (1973).
18. D. E. Aspnes and A. A. Studna, "Dielectric functions and Optical Parameters of Si, Ge, GaP, Ga As, Ga Sb, In P, InAs, and InSb from 1.5 to 6.0 eV," Phys. Rev. B **27,** 985 (1983).


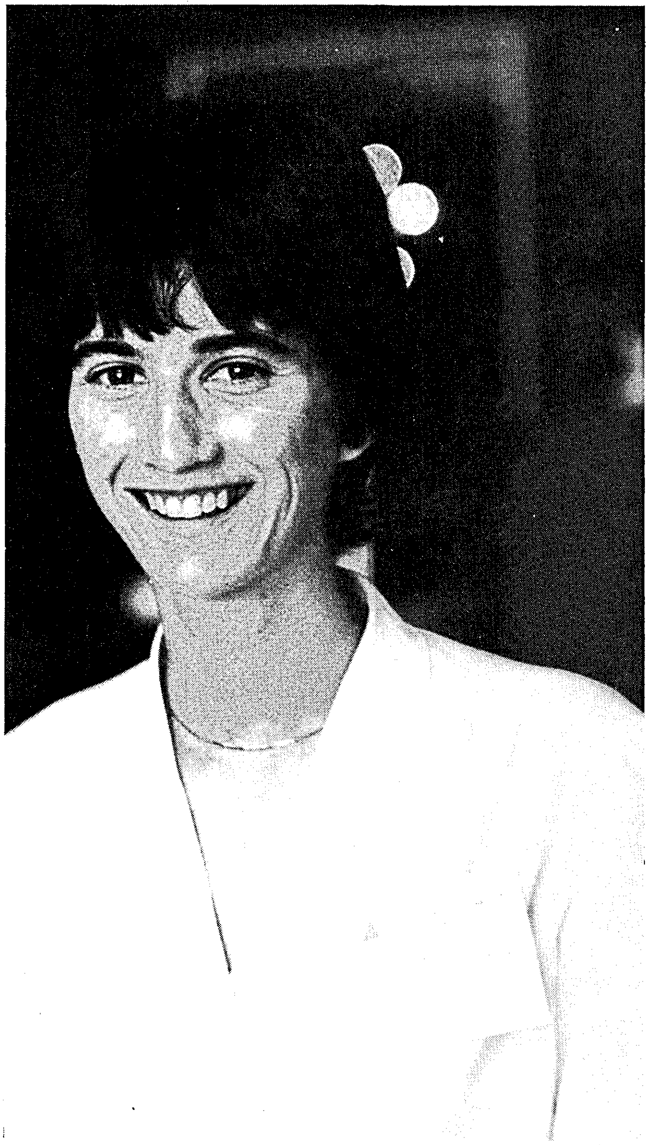

Kristina M. Johnson, of Trinity College, Dublin, photographed by W. J. Tomlinson, of Bell Communications Research, during the 1984 OSA Annual Meeting held in San Diego.